Impurity tolerance of polymer solar cells: The crucial role of palladium catalyst and its ligands

Gilles Roche, Lucas Viollet, Nicolas Penin, Tanguy Jousselin-Oba, Chloé Dindault, Laurence Vignau, Sylvain Chambon, Lionel Hirsch, Pierre-Antoine Bonnardel, Sébastien Taillemite, et al.

Solar Energy Materials & Solar Cells xxx (xxxx) xxx

Contents lists available at ScienceDirect

Solar Energy Materials and Solar Cells

journal homepage: www.elsevier.com/locate/solmat

Impurity tolerance of polymer solar cells: The crucial role of palladium catalyst and its ligands

Gilles H. Roche [a,*], Lucas Viollet [a], Nicolas Penin [c], Tanguy Jousselin-Oba [a,b], Chloé Dindault [a,b], Laurence Vignau [a], Sylvain Chambon [a], Lionel Hirsch [a], Pierre-Antoine Bonnardel [b], Sebastien Taillemite [b], Guillaume Wantz [a,**]

[a] Univ. Bordeaux, CNRS, Bordeaux INP, Laboratoire IMS, UMR 5218, F-33400, Talence, France
[b] SEQENS SAS – 21, chemin de la Sauvegarde, CS 33167, 69134, Ecully, France
[c] CNRS, Univ. Bordeaux, Bordeaux INP, ICMCB, UMR5026, F-33608, Pessac, France

ARTICLE INFO

Keywords:
Catalyst traces
Impurities
Organic solar cells
Ligand
Stability

ABSTRACT

Polymer photovoltaic solar cells based on PTQ10:IT4F were fabricated and characterized with voluntary contamination of several impurities in various amounts. Impurities were selected as related to the Stille coupling reagents: in particular palladium catalysts and their respective ligands. Below a concentration of 300 ppm, the pristine device efficiencies were not significantly affected for any of the studied compounds. The degradation patterns under accelerated light soaking were not modified either. For higher impurities amounts (>300 ppm), $Pd(PPh_3)_4$ catalyst shows a strong poisoning effect on both pristine device performances and operating stability. Interestingly, we demonstrate that not only the metallic center of the catalytic complex, but also the ligands can play a role on the organic solar cells performances.

1. Introduction

Organic photovoltaic (OPV) solar cells are approaching the maturity in the light of large-scale printing solar panel deployment. Impressive power conversion efficiencies (PCE) in single-junction have been achieved in laboratory with over 19% at the cell level [1–3] and over 14% [4,5] at module level on a laboratory scale. High quality materials are essential to achieve high performance OPV devices [6]. OPV solar cells are usually based on an active layer composed of a bulk heterojunction (BHJ) made of two semiconducting materials. One of these materials is an electron donor, mainly a polymer and less frequently a solution-processable small molecule [7,8]. The second material is an electron acceptor, initially a fullerene derivative [9], and currently, mostly a non-fullerene acceptor (NFA) [10–12] or rarely NFA-inspired polymers [13–15]. From a chemical synthesis point of view, small molecules and fullerenes are small repeated units easier to purify and reproduce than polymers. Column chromatography and recrystallisation are common process that allows to limit residue accumulation and minimize batch-to-batch variation. On the other hand, polymers are usually prepared from catalyzed polycondensation reaction, generating long chains whose length variation are inherent to reaction conditions. These long chains of different length, do not allow easy purification process which lead to residues accumulation, in particular those from reagents introduction. With a lack of purification strategy, their presence in the active layer can induce severe losses of device performances. Indeed, Bracher et al. demonstrated that remaining metallic nanoparticles from catalyst can induce current shunts within the device [16]. Liu et al. showed polymer oxidation assisted by palladium [17]. Saeki et al., Camaioni et al. and Schopp et al., reported that catalyst remaining traces can alter organic photovoltaic devices by affecting charge carriers mobility [18–20]. Here we show that not only catalysts but also catalyst ligands can affect OPV solar cells. To provide a global insight concerning reaction residues, a series of compounds has been studied and classified as detrimental or inert towards device performances.

2. Discussion

For this study, the polymer PTQ10[1] has been chosen [21]. This

* Corresponding author.
** Corresponding author.
E-mail addresses: gilles.roche@u-bordeaux.fr (G.H. Roche), guillaume.wantz@ims-bordeaux.fr (G. Wantz).

[1] PTQ10: poly[(thiophene)-alt-(6,7-difluoro-2-(2-hexyldecyloxy)quinoxaline)].

https://doi.org/10.1016/j.solmat.2024.112760
Received 15 November 2023; Received in revised form 12 February 2024; Accepted 16 February 2024

polymer presents a low synthetic complexity and promising performances [2] which fits with large scale industrial chemistry requirements.

Two synthetic paths were reported for this polymer (the first is depicted on Fig. 1 and the second [22] in Fig. 1S). We focused on their last common polymerization step, a Stille coupling where stannylated thiophenes react with a bis-bromo-alkyl-oxyquinoxaline (**3**). To estimate residues impacts coming from this step on OPV performances, the PTQ10 polymer was blended with the non-fullerene acceptor IT4F[2] [23]. This NFA is in accordance with the energetic levels of PTQ10 (Fig. 2a). This photoactive blend was introduced in the following inverted architecture: of ITO/ZnO/BHJ/MoO_3/Ag, where ZnO is the electron collector and MoO_3 the hole one. Device fabrication is detailed in supporting information. Fig. 2 depict an averaged typical current-voltage characteristic and optoelectronic properties, of this kind of solar cell.

First, the PTQ10 batch was characterized in term of purity. Trace elemental analyses were performed in order to evaluate the synthesis residues in the polymer. Palladium (Pd), Tin (Sn) and Phosphorus (P) contents have been measured on the as-received polymer using ICP-OES (Inductive Coupled Plasma Optical Emission Spectrometry). The analysis showed a Pd content of 18 ppm, which can be considered as low especially compared to previous work where concentrations of over thousands ppm were reported [16,19]. Unexpectedly, the Tin content was 874 ppm. Such a high concentration was unexpected and maybe related to reagent residues (step iii. in Fig. 1) but also from Sn-ending polymer chains. Indeed, during the polymerization condensation reaction (Fig. S2) Bromo-trimethylstanyl chemical should be released. This highly reactive compound, should be rapidly converted into trimethylstannylol or methoxytrimethylstannane during methanol precipitation purification process performed in air. Both are small molecules, highly soluble and with a high vapor pressure as stannylated compounds. So, their presence in the polymer would be really surprising and thus very unfortunate. The second possibility of tin residue source is in the non-capping of the polymer chains. The Trimethylstanyl function is relatively fragile (usually easy to hydrolyze). But, with organic semiconductor polymer folding properties [24], protection of this function in a polymer matrix is more credible. All these aspects may reveal the necessity of an end-capping procedure or a special process to help the hydrolysis for a better control of the polymers on remaining tin aspect. And this result itself is highly relevant to set the specifications of the purity requirements. Finally, phosphorus content was found to be below the detection level of the ICP-OES measurement.

OPV devices have been characterized in terms of performances on freshly prepared samples. In order to understand the impact of a probable contaminations, seven different compounds were investigated as impurities and introduced deliberately in the active layer at different concentrations. Indeed, according to the PTQ10 catalytic polymerization cycle depicted in Fig. S2, the most abundant impurities that could remain after polymerization condensation are catalysts, catalyst ligands, stannylated compounds, and brominated compounds.

Tetrakis(triphenylphosphine)palladium(0) ($Pd(PPh_3)_4$), one of the most used catalyst in pallado-catalyzed C-C cross coupling in organic chemistry, was selected as an impurity to study. This pollutant has been previously investigated by various teams [16,17,20,25]. Schopp et al. reported a study for a BHJ composed of PTB7-Th/IOTIC-4F [20]. It was observed a considerable detrimental effect on PCE at 3 %wt Pd of catalyst vs polymer which corresponds to a Pd contamination at 2760 ppm with respect to the donor. To picture the order of magnitude, in the literature, an usual contamination of 2000–3000 ppm Pd was described in different polymers [16,19]. As a consequence, we studied the addition of $Pd(Ph_3)_4$ of respectively 0, 300, 600, 1200 and 2500 ppm in the active layer of the OPV cells, keeping in mind that our baseline is at 18 ppm. $Pd(PPh_3)_4$ represents a source of palladium where the metal oxidation state is (0). This metallic complex is also in a dynamic equilibrium that can release triphenylphosphine (PPh_3) ligand to provide access to the reactive Pd atom during the polymerization reaction. It is then also important to run control experiments using PPh_3 as a potential contaminant to understand if damages are caused by the metal itself or by its ligands. To provide a fulfil insight on this aspect, it would be logic to introduce also metallic Pd, which is impossible (Pd atoms agglomerate to generate black palladium). That is also why investigating another source of Palladium (0) was relevant. Tris(dibenzylideneacetone)dipalladium(0) ($Pd_2(dba)_3$) in addition with PPh_3 is commonly used to generate *in situ* $Pd(PPh_3)_4$ catalyst [22]. $Pd_2(dba)_3$ addition was also studied with control experiment with (dibenzylideneacetone (dba). To complete this aspect, it was worthy to examine a source Pd where the metal oxidation state is (II).Indeed, in presence of a reducer Pd (II) can also be used in the case of Suzuki reaction in polycondensation polymerization to generate Pd(0) catalyst complex *in situ* [26]. For this reason, a Palladium(II) acetate ($Pd(OAc)_2$) was chosen, as well as acetic acid (AcOH) in control experiments. Finally, as last residue, we also introduced on purpose bistrimethylstanylthiophene (($Me_3Sn)_2$-Thio) as a source of Tin. The chemical structures of these compounds are displayed in inset of graphs of Fig. 3a.

3. Initial performances of OPV cells: impact of the contaminants

The impact of the considered impurities on PV efficiency for pristine cells (*i.e.* at t0) is shown on Fig. 3b–e. First, one can observe on Fig. 3b, $Pd(PPh_3)_4$ introduction at concentrations superior to 300 ppm is detrimental for the PCE. Indeed, PTQ10:IT4F pristine devices exhibit PCE around 9.2%, whereas with 2500 ppm of $Pd(PPh_3)_4$ it drops to 6.3% (a 30% loss). Nikiforov et al. reported that below 1 wt% Pd (= 920 ppm Pd), the damage on the performances of PTB7:PCBM devices were not significative [25]. They considered that $Pd(PPh_3)_4$ addition does not affect device performance until the Pd concentration became larger than the initial Pd concentration. Since here, the initial concentration is very low (18 ppm), far below 1 wt% Pd, a slight increase in PCE (0.5%), associated to an increase of FF (see Fig. S3) is observed up to 300 ppm. This benefic trend is similar to the use of additives, like the common diiodooctane (DIO) [27] which improves initial OPV performance. So "additive effect" summarize well this phenomenon. Interestingly, at 0.75 wt% Pd (= 690 ppm Pd), Schopp et al. observed the same increase of the performances [20]. They also noticed a slight increase of coherence lengths describing PTB7-Th lamellar stacking, suggesting that this improvement could be explained by a little benefice in polymer chain ordering at low contaminant concentration. Concerning the following 30 % loss, such performance decrease is consistent with the work reported by Schopp et al. where 44% of PCE were lost in PTB7-Th:IOTIC-4F solar cells [20]. These performances losses are principally due to a considerable impact on the current density (J_{SC}, as can be seen in Fig. S3), with a drop from 17.5 mA/cm^2 for the non-polluted condition down to 14.2 mA/cm^2 for 2500 ppm, while the open circuit voltage (Voc) remains extremely stable with the increasing concentration of Pd (Fig. S3d). This loss in Jsc is also observed on the External Quantum Efficiency measurements (Fig. S11a). To understand how the catalyst hampers device efficiency, thin film morphology was imaged by AFM (Atomic Force Microscopy) and charge carrier mobility was extracted from SCLC (Space Charged Limited Current) characterizations of hole only and electron only devices. No clear and significant change in the height and phase BHJs AFM images was observed upon addition of the $Pd(PPh_3)_4$ suggesting that introduction of 300 ppm or 2500 ppm of Pd, via $Pd(PPh_3)_4$, in the BHJ does not affect the active layer morphology (see Figs. S12–S14) as already reported [20]. Concerning electron mobility obtained by SCLC, comparable mobility (see Table 1) around 2.2×10^{-4} cm^2 V^{-1} s^{-1} was observed on pristine samples and with 300

[2] IT4F: 3,9-bis(2-methylene-((3-(1,1-dicyanomethylene)-6,7-difluoro)-indanone))-5,5,11,11-tetrakis(4-hexylphenyl)-dithieno[2,3-*d*:2′,3′-*d*′]-*s*-indaceno [1,2-*b*:5,6-*b*′]dithiophene, (Molecular structure in SI).

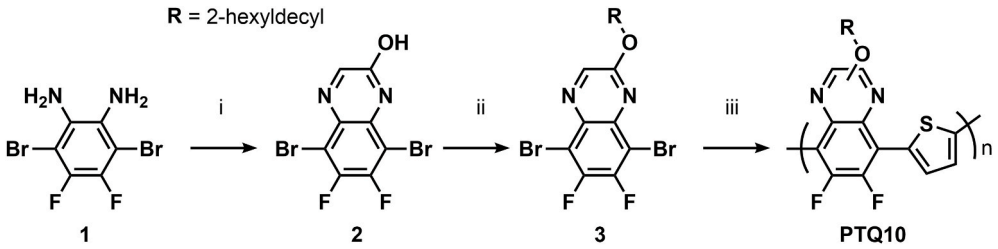

Fig. 1. First synthesis of PTQ10 described by Sun et al. [21], reaction conditions: i: Glyoxylic acid, AcOH, r.t.; ii: 1-bromo-2-hexyldecane, ; iii: 2,5-bis(trimethylstannyl)thiophene, $Pd(PPh_3)_4$, toluene, reflux.

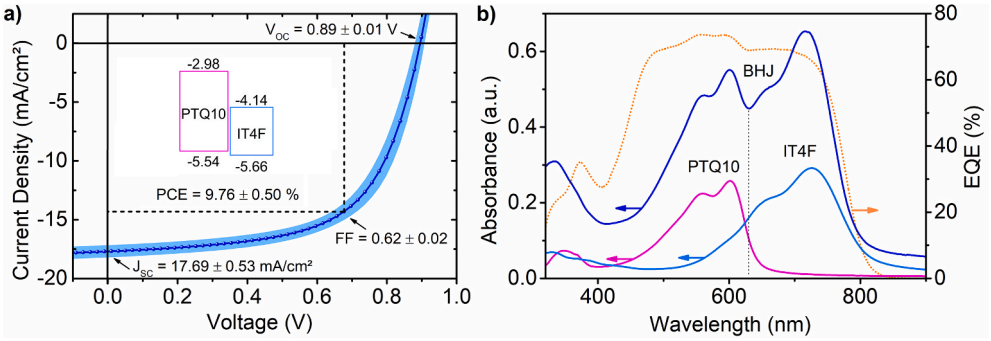

Fig. 2. a) Typical JV curve of PQT10:IT4F-based devices (average of 64 devices), with energetic levels (expressed in eV). JV curves with deep blue dots and lines indicating the averaged curve, shades indicating the standard deviations, dash indicates were PCE max is generally obtained; b) Absorbance of a pristine PTQ10 (pink line), pristine IT4F (blue line) and PTQ10:IT4F (ratio 1:1.2) BHJ (purple line) thin films and external quantum efficiency (EQE, orange dotes).

and 2500 ppm of introduced palladium. The pollutant are not significantly affecting the electron mobility. On the opposite, the hole mobility is significantly affected by the addition of $Pd(PPh_3)_4$. With 300 ppm impurity the hole mobility decreased of about half of the pristine value, from 5.2×10^{-5} to 2.7×10^{-5} $cm^2 V^{-1} s^{-1}$. The addition of 2500 ppm of Pd generates a loss of one order of magnitude, down to 5.7×10^{-6} $cm^2 V^{-1} s^{-1}$. Plotting the current-voltage curves of hole only devices in logarithm scale demonstrated a characteristic trap assisted regime (see Fig. 4) [28]. Due to the pollution with $Pd(PPh_3)_4$ even at 300 ppm level (see Fig. S16). This trapping mechanism was not observed by Shopp et al. [20] observing a preserved hole mobility in their study based on a different material system. Our observation underlines that impurity mechanisms require advanced studies for each type of active layer. Our experiment illustrates once again that, like previous studies of Nikiforov et al. and Schopp et al., but in a different active layer: PTQ10:IT4F, large amount of remaining palladium catalyst (>300 ppm) have a detrimental effect.

As underlined previously, catalyst complexes are not fully covalent entities, ligands are labile and can coordinate/uncoordinate very quickly, this aspect was of high importance to study. With that in mind, investigating the introduction effect of the same amounts of the ligand PPh_3, without the palladium itself seemed to be an appropriate control experiment (Fig. 3b). Surprisingly, a very similar detrimental effects with the ligand compared to the complete palladium catalyst. Once again AFM measurements showed no significative modifications (see Fig. S15) and comparable trap assisted mechanism were observed with SCLC measurements (see Fig. S17) suggesting the importance of this molecule in hole trap creation. Therefore, the metallic atom itself cannot be the only moiety responsible for device PCE losses. In order to determine if the damages were only due to the phosphine part, the impact of another source of Pd(0): $Pd_2(dba)_3$, on the OPV performances was studied. With $Pd_2(dba)_3$ as contaminant, a similar behavior is again observed (Fig. 3c): starting with a PCE at 10.2%, the same "additive effect" was observed up to 100 ppm (with 0.8% of PCE increase), followed by PCE losses above 300 ppm to reach 7% (31% loss). Then we used the same strategy as before, *ie* keeping the dba ligand without the Pd. No clear dependence of PCE on dba concentration was observed. As a consequence, in this experiment, the palladium clearly seems to be responsible for the PCE loss. For further insight, a source of palladium (II): $Pd(OAc)_2$, less used as a catalyst, was investigated (Fig. 3d). This compound with an initial PCE of 9.6% generated, once again, a small increase in performance (0.2% of PCE) up to 300 ppm followed by a less pronounced decrease of performance (20% loss). Note that the acetic acid control experiment did not here again show any PCE loss. As a conclusion, the three palladium containing catalysts (metallic or ionic) are showing similar behavior of PCE losses on pristine devices as well as the phosphine ligands. This confirms that, not only the metallic Pd, but also the phosphine ligands can impact similarly the solar cells.

As remaining phosphine has to be considered, its degree of oxidation can also be a relevant parameter. That is why, we proceeded to a complementary experiment with the introduction of triphenylphosphine oxide in the same amount than in PPh_3 experiment (Fig. S3). And remarkably triphenylphosphine oxide does not exhibit any adverse effect on the OPV efficiency. This experiment highlights that the bulkiness of triphenylphosphine groups does not impact the photovoltaic performances, suggesting that the active layer morphology is not impacted. On the contrary, it demonstrates an important point: the doublet of the phosphine is the key parameter able to damage solar cells performances.

Finally, the impact of stannylated compound $(Me_3Sn)_2$-Thio on the initial performances was investigated. This source of tin, does not affect the photovoltaic properties even for high content, up to 2500 ppm (Fig. 3e). Although surprising, this result should be put in perspective since already 874 ppm of tin is present in the as-received polymer (from our ICP-OES analysis). We can still admit that the introduction of up to 2500 ppm of tin (four times tin residues) should be enough to initiate any impact on devices performances, which is not the case. Tin contamination seems to have globally no adverse effect until 3300 ppm on the solar cell which is encouraging.

4. Impurities impact on devices aging

To evaluate the stability of the devices under light soaking,

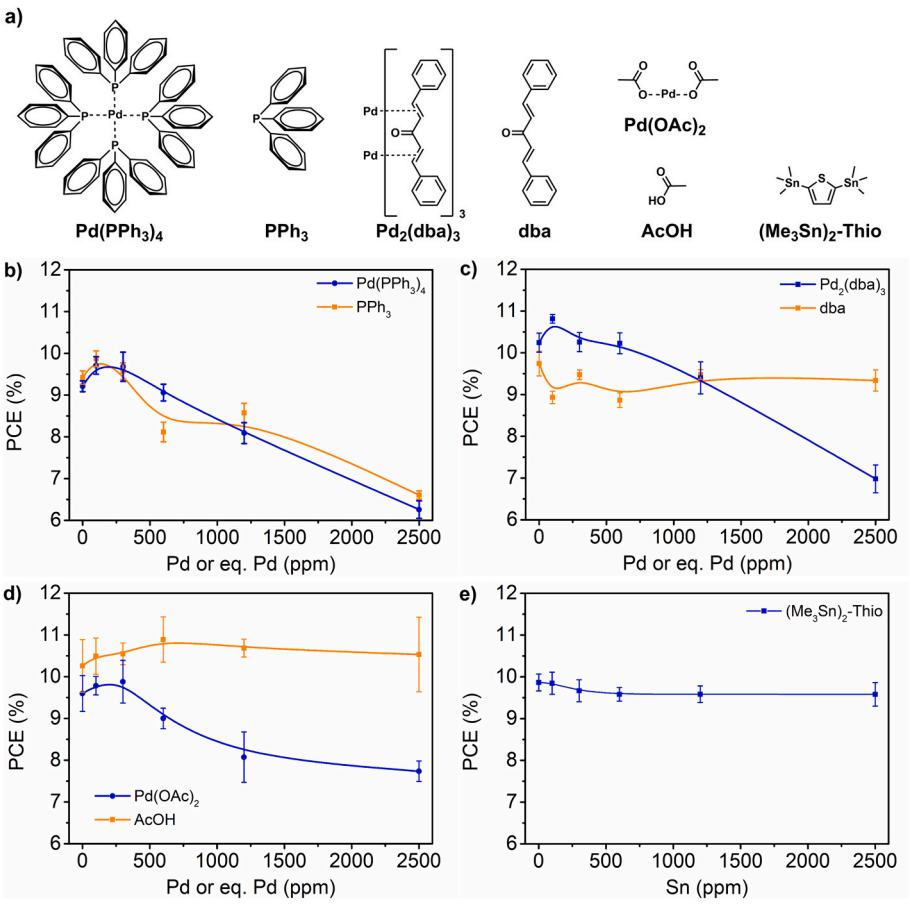

Fig. 3. (a) Chemical structures of the studied molecules. (b–e) Dependence of PCEs of PTQ10:IT4F pristine cells with the introduced concentration of impurity for a) $Pd(PPh_3)_4$ and its ligand PPh_3, b) $Pd_2(dba)_3$ and its ligand dba, c) $Pd(OAc)_2$ and AcOH and d) $(Me_3Sn)_2$-Thio. Error bars indicate standard deviation on a minimum of 8 cells. See Figs. S3–S6 for different photovoltaic parameters (Jsc, Voc, FF).Note that zero means no voluntary introduction, i.e. pristine materials with a measured residual Pd content of 18 ppm, Sn content of 874 ppm and P content 0 ppm. (b) $Pd(PPh_3)_4$ and PPh_3; (c) $Pd_2(dba)_3$ and dba; (d) $Pd(OAc)_2$ and AcOH; (e) $(Me_3Sn)_2$-Thio. Note also that, for PPh_3, dba, and AcOH, the introduced amounts are exactly the same amount than in case of corresponding catalyst introduction without Palladium for comparison. That is why you can read equivalent Pd ppm ("eq. Pd" ppm).

Table 1
Mobility of electrons (e^-) and holes (h^+) obtained by SCLC measurements.

Mobility ($cm^2.V^{-1}.s^{-1}$)		
Pd (ppm)	e^-	h^+
0 ppm	2.2×10^{-4}	5.2×10^{-5}
300 ppm	2.2×10^{-4}	2.7×10^{-5}
2500 ppm	2.1×10^{-4}	5.7×10^{-6}
2500 eq ppm (PPh_3)	1.9×10^{-4}	7.7×10^{-6}

accelerated ageing of samples has been performed under 1.5 sun in a chamber with a controlled temperature of 50 °C. For the devices contaminated, the most representative cases were selected: 0 ppm, as reference, 300 ppm, for the noticed "additive effect" and 2500 ppm, where damages were obvious. Fig. 5a shows the evolution of the PCE for the seven impurities at a concentration of 300 ppm or equivalent.

For low concentration (300 ppm or eq.), the initial PCEs of the different samples were very similar, and in order to facilitate the comparison between the samples, the evolution upon ageing of normalized PCEs are presented (See in Fig. S7 for non-normalized values). All OPV devices show the same degradation kinetics as the control device, regardless of the type of contaminant. After 30 h of accelerated ageing, all samples still have 80% of initial performances. The evolution of the different photovoltaic parameters (Jsc, Voc, FF) are presented in Figs. S7 and S8. From these results, it seems that low concentrations of impurities (below 300 ppm or eq) do not affect significantly the degradation

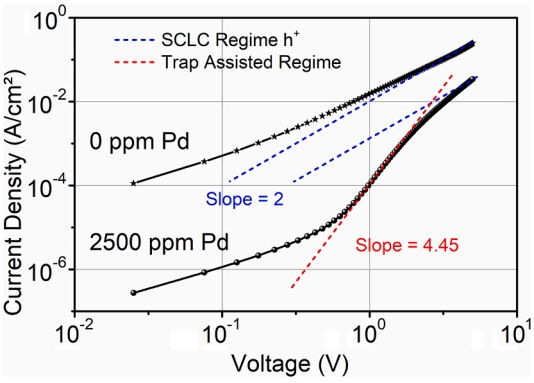

Fig. 4. SCLC measurements of hole only devices containing 0 and 2500 ppm de Pd.

kinetics and in particular the burn-in.

For higher concentration (2500 ppm or eq.), normalized PCEs are shown on Fig. 5b (See in Fig. S9 for non-normalized values). For most of the contaminants, except $Pd(PPh_3)_4$ and $Pd(OAc)_2$, PCEs are following the same degradation kinetics observed previously for low concentrations. The evolution of the different photovoltaic parameters (Jsc, Voc, FF) are presented in Figs. S9 and S10. $Pd(OAc)_2$, which has a slightly better FF maintained, is slowing devices degradation. At the opposite, Pd

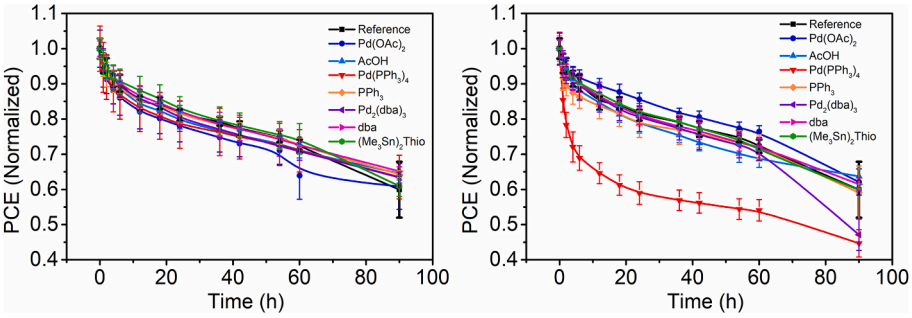

Fig. 5. a) and b) represent normalized PCEs of OPV devices at 300 and 2500 ppm Pd or eq respectively. $Pd(OAc)_2$ (deep blue line), AcOH (blue line), $Pd(PPh_3)_4$ (red line), PPh_3 (orange line), $Pd_2(dab)_3$ (violet line), dba (pink line) and $(Me_3Sn)_2$-Thio green short dash, compared to the reference without introduced impurities (black line) under light soaking. Error bars indicate standard deviations.

$(PPh_3)_4$, due to a combination of severe damage on FF and J_{SC}, seriously damages the solar cells. As this catalyst is well known to be light sensitive, it means that, at high concentration, due to light exposition, highly reactive entities are released in the active layer accelerating the aging of the cells.

5. Conclusion

During this study we highlight that Stille reaction impurities can have an impact on pristine organic solar cells performances and on the stability under light soaking. For PTQ10:IT4F active layer we demonstrated that $Pd(PPh_3)_4$ but also its phosphine ligand PPh_3 severely affect photovoltaic performances at high pollution content (> 300 ppm). At low concentration (≈ 300 ppm) a slight improvement of the performances can be observed which might be related to morphology changes. Under light soaking, for low concentration of residues (≈ 300 ppm), no significant changes were observed, the degradation kinetics remaining similar to that of the reference device. At high concentration (2500 ppm), the different contaminants did not show a significant impact on the stability of the devices, except for palladium catalysts. In particular, $Pd(PPh_3)_4$ clearly shows a detrimental effect on the solar cells performances, mainly due to a strong decrease of FF and Jsc. According to our study, tin residues are inert below 3300 ppm and a palladium residues content below 300 ppm is an acceptable threshold. However, we did not investigate the mix of impurities. Therefore, we have no information related to the cocktail effect. Thus, we can only recommend to have the lowest level of residues in OSC polymers. Finally, this study clearly points out the necessity to carefully purify the raw materials for OPV, systematically check their contamination level through trace residue analysis, proceed end-capping and set specifications of the purity. Such effort would improve the materials quality to enable high efficiency and stable organic solar cells in the future.

Funding

This work was supported by Agence Nationale de la Recherche (ANR) [Labcom SPRINT ANR-19-LCV1-0006, 2019].

CRediT authorship contribution statement

Gilles H. Roche: Writing – original draft, Supervision, Investigation, Conceptualization. **Lucas Viollet:** Investigation. **Nicolas Penin:** Methodology. **Tanguy Jousselin-Oba:** Writing – review & editing. **Chloé Dindault:** Writing – review & editing. **Laurence Vignau:** Writing – review & editing. **Sylvain Chambon:** Writing – review & editing. **Lionel Hirsch:** Writing – review & editing. **Pierre-Antoine Bonnardel:** Writing – review & editing. **Sebastien Taillemite:** Writing – review & editing, Project administration. **Guillaume Wantz:** Writing – review & editing, Supervision, Project administration, Funding acquisition, Conceptualization.

Declaration of competing interest

The authors declare that they have no known competing financial interests or personal relationships that could have appeared to influence the work reported in this paper.

Data availability

Data will be made available on request.

Appendix A. Supplementary data

Supplementary data to this article can be found online at https://doi.org/10.1016/j.solmat.2024.112760.

References

[1] L. Zhu, M. Zhang, J. Xu, C. Li, J. Yan, G. Zhou, W. Zhong, T. Hao, J. Song, X. Xue, Z. Zhou, R. Zeng, H. Zhu, C.C. Chen, R.C.I. MacKenzie, Y. Zou, J. Nelson, Y. Zhang, Y. Sun, F. Liu, Single-junction organic solar cells with over 19% efficiency enabled by a refined double-fibril network morphology, Nat. Mater. 21 (2022) 656–663, https://doi.org/10.1038/s41563-022-01244-y.

[2] X. Kong, J. Zhang, L. Meng, C. Sun, X. Jiang, J. Zhang, C. Zhu, G. Sun, J. Li, X. Li, Z. Wei, Y. Li, Low-Cost and high-performance polymer solar cells with efficiency insensitive to active-layer thickness, CCS Chem. 23 (2023) 1–11, https://doi.org/10.31635/ccschem.023.202302720.

[3] J. Fu, P.W.K. Fong, H. Liu, C.S. Huang, X. Lu, S. Lu, M. Abdelsamie, T. Kodalle, C. M. Sutter-Fella, Y. Yang, G. Li, 19.31% binary organic solar cell and low non-radiative recombination enabled by non-monotonic intermediate state transition, Nat. Commun. 14 (2023), https://doi.org/10.1038/s41467-023-37526-5.

[4] S. Dong, T. Jia, K. Zhang, J. Jing, F. Huang, Single-component non-halogen solvent-processed high-performance organic solar cell module with efficiency over 14, Joule 4 (2020) 2004–2016, https://doi.org/10.1016/j.joule.2020.07.028.

[5] X. Dong, Y. Jiang, L. Sun, F. Qin, X. Zhou, X. Lu, W. Wang, Y. Zhou, Large-area organic solar modules with efficiency over 14, Adv. Funct. Mater. (2021) 2110209, https://doi.org/10.1002/adfm.202110209.

[6] Ö. Usluer, M. Abbas, G. Wantz, L. Vignau, L. Hirsch, E. Grana, C. Brochon, E. Cloutet, G. Hadziioannou, Metal residues in semiconducting polymers: impact on the performance of organic electronic devices, ACS Macro Lett. 3 (2014) 1134–1138, https://doi.org/10.1021/mz500590d.

[7] B. Kan, Y. Kan, L. Zuo, X. Shi, K. Gao, Recent progress on-all-small molecule organic solar cells using -small-molecule nonfullerene acceptors, InfoMat 3 (2021) 175–200, https://doi.org/10.1002/inf2.12163.

[8] J. Ge, L. Xie, R. Peng, Z. Ge, Organic photovoltaics utilizing small-molecule donors and Y-series nonfullerene acceptors, Adv. Mater. 35 (2023) 1–19, https://doi.org/10.1002/adma.202206566.

[9] S. Li, C.-Z. Li, M. Shi, H. Chen, New phase for organic solar cell research: emergence of Y-series electron acceptors and their perspectives, ACS Energy Lett. 5 (2020) 1554–1567, https://doi.org/10.1021/acsenergylett.0c00537.

[10] H. Wang, J. Cao, J. Yu, Z. Zhang, R. Geng, L. Yang, W. Tang, Molecular engineering of central fused-ring cores of non-fullerene acceptors for high-efficiency organic solar cells, J. Mater. Chem. A 7 (2019) 4313–4333, https://doi.org/10.1039/c8ta12465e.

[11] S.P. Singh Suman, Impact of end groups on the performance of non-fullerene acceptors for organic solar cell applications, J. Mater. Chem. A 7 (2019) 22701–22729, https://doi.org/10.1039/c9ta08620j.

[12] Y. Pan, X. Zheng, J. Guo, Z. Chen, S. Li, C. He, S. Ye, X. Xia, S. Wang, X. Lu, H. Zhu, J. Min, L. Zuo, M. Shi, H. Chen, A new end group on nonfullerene acceptors endows efficient organic solar cells with low energy losses, Adv. Funct. Mater. 32 (2022), https://doi.org/10.1002/adfm.202108614.

[13] Q. Wu, W. Wang, Y. Wu, Z. Chen, J. Guo, R. Sun, J. Guo, Y. Yang, J. Min, High-performance all-polymer solar cells with a pseudo-bilayer configuration enabled by a stepwise optimization strategy, Adv. Funct. Mater. 31 (2021) 1–9, https://doi.org/10.1002/adfm.202010411.

[14] H. Fu, Y. Li, J. Yu, Z. Wu, Q. Fan, F. Lin, H.Y. Woo, F. Gao, Z. Zhu, A.K.Y. Jen, High efficiency (15.8%) all-polymer solar cells enabled by a regioregular narrow bandgap polymer acceptor, J. Am. Chem. Soc. 143 (2021) 2665–2670, https://doi.org/10.1021/jacs.0c12527.

[15] J. Guo, T. Wang, Y. Wu, R. Sun, Q. Wu, W. Wang, H. Wang, X. Xia, X. Lu, T. Wang, J. Min, Revealing the microstructure-related light-induced degradation for all-polymer solar cells based on regioisomerized end-capping group acceptors, J. Mater. Chem. C 10 (2022) 1246–1258, https://doi.org/10.1039/d1tc05030c.

[16] C. Bracher, H. Yi, N.W. Scarratt, R. Masters, A.J. Pearson, C. Rodenburg, A. Iraqi, D.G. Lidzey, The effect of residual palladium catalyst on the performance and stability of PCDTBT:PC70BM organic solar cells, Org. Electron. 27 (2015) 266–273, https://doi.org/10.1016/j.orgel.2015.10.001.

[17] L. Liu, B. Yang, H. Zhang, S. Tang, Z. Xie, H. Wang, Z. Wang, P. Lu, Y. Ma, Role of tetrakis(triphenylphosphine)palladium(0) in the degradation and optical properties of fluorene-based compounds, J. Phys. Chem. C 112 (2008) 10273–10278, https://doi.org/10.1021/jp8010316.

[18] A. Saeki, M. Tsuji, S. Seki, Direct evaluation of intrinsic optoelectronic performance of organic photovoltaic cells with minimizing impurity and degradation effects, Adv. Energy Mater. 1 (2011) 661–669, https://doi.org/10.1002/aenm.201100143.

[19] N. Camaioni, F. Tinti, L. Franco, M. Fabris, A. Toffoletti, M. Ruzzi, L. Montanari, L. Bonoldi, A. Pellegrino, A. Calabrese, R. Po, Effect of residual catalyst on solar cells made of a fluorene-thiophene- benzothiadiazole copolymer as electron-donor: a combined electrical and photophysical study, Org. Electron. 13 (2012) 550–559, https://doi.org/10.1016/j.orgel.2011.12.005.

[20] N. Schopp, V.V. Brus, J. Lee, A. Dixon, A. Karki, T. Liu, Z. Peng, K.R. Graham, H. Ade, G.C. Bazan, T.Q. Nguyen, Effect of palladium-tetrakis(triphenylphosphine) catalyst traces on charge recombination and extraction in non-fullerene-based organic solar cells, Adv. Funct. Mater. 31 (2021), https://doi.org/10.1002/adfm.202009363.

[21] C. Sun, F. Pan, H. Bin, J. Zhang, L. Xue, B. Qiu, Z. Wei, Z.G. Zhang, Y. Li, A low cost and high performance polymer donor material for polymer solar cells, Nat. Commun. 9 (2018) 1–10, https://doi.org/10.1038/s41467-018-03207-x.

[22] J.J. Rech, J. Neu, Y. Qin, S. Samson, J. Shanahan, R.F. Josey, H. Ade, W. You, Designing simple conjugated polymers for scalable and efficient organic solar cells, ChemSusChem 14 (2021) 3561–3568, https://doi.org/10.1002/cssc.202100910.

[23] W. Zhao, S. Li, H. Yao, S. Zhang, Y. Zhang, B. Yang, J. Hou, Molecular optimization enables over 13% efficiency in organic solar cells, J. Am. Chem. Soc. 139 (2017) 7148–7151, https://doi.org/10.1021/jacs.7b02677.

[24] T.J. Fauvell, T. Zheng, N.E. Jackson, M.A. Ratner, L. Yu, L.X. Chen, Photophysical and morphological implications of single-strand conjugated polymer folding in solution, Chem. Mater. 28 (2016) 2814–2822, https://doi.org/10.1021/acs.chemmater.6b00734.

[25] M.P. Nikiforov, B. Lai, W. Chen, S. Chen, R.D. Schaller, J. Strzalka, J. Maser, S. B. Darling, Detection and role of trace impurities in high-performance organic solar cells, Energy Environ. Sci. 6 (2013) 1513–1520, https://doi.org/10.1039/c3ee40556g.

[26] C. Amatore, A. Jutand, Anionic Pd(0) and Pd(II) intermediates in palladium-catalyzed heck and cross-coupling reactions, Acc. Chem. Res. 33 (2000) 314–321, https://doi.org/10.1021/ar980063a.

[27] M.T. Seifrid, S.D. Oosterhout, M.F. Toney, G.C. Bazan, Kinetic versus thermodynamic orientational preferences for a series of isomorphic molecular semiconductors, ACS Omega 3 (2018) 10198–10204, https://doi.org/10.1021/acsomega.8b01435.

[28] V.M. Le Corre, E.A. Duijnstee, O. El Tambouli, J.M. Ball, H.J. Snaith, J. Lim, L.J. A. Koster, Revealing charge carrier mobility and defect densities in metal halide perovskites via space-charge-limited current measurements, ACS Energy Lett. 6 (2021) 1087–1094, https://doi.org/10.1021/acsenergylett.0c02599.